TISSUE ENGINEERING: Part C
Volume 22, Number 4, 2016

DOI: 10.1089/ten.tec.2015.0465

termis
Tissue Engineering
& Regenerative Medicine
International Society

METHODS ARTICLE

Physiologically Low Oxygen Enhances Biomolecule Production and Stemness of Mesenchymal Stem Cell Spheroids

Emily Shearier, Qi Xing, Zichen Qian, and Feng Zhao, PhD

Multicellular human mesenchymal stem cell (hMSC) spheroids have been demonstrated to be valuable in a variety of applications, including cartilage regeneration, wound healing, and neoangiogenesis. Physiological relevant low oxygen culture can significantly improve *in vitro* hMSC expansion by preventing cell differentiation. We hypothesize that hypoxia-cultured hMSC spheroids can better maintain the regenerative properties of hMSCs. In this study, hMSC spheroids were fabricated using hanging drop method and cultured under 2% O_2 and 20% O_2 for up to 96 h. Spheroid diameter and viability were examined, as well as extracellular matrix (ECM) components and growth factor levels between the two oxygen tensions at different time points. Stemness was measured among the spheroid culture conditions and compared to two-dimensional cell cultures. Spheroid viability and structural integrity were studied using different needle gauges to ensure no damage would occur when implemented *in vivo*. Spheroid attachment and integration within a tissue substitute were also demonstrated. The results showed that a three-dimensional hMSC spheroid cultured at low oxygen conditions can enhance the production of ECM proteins and growth factors, while maintaining the spheroids' stemness and ability to be injected, attached, and potentially be integrated within a tissue.

Introduction

One of the tissue engineering approaches is the growth of cells into spheroids. In spheroid culture, a small number of cells grow to form a self-supported aggregate, which is free from foreign materials.[1] Self-assembly of these cell populations arises from intracellular adhesiveness and energy minimization.[2–4]The presence of extracellular matrix (ECM) proteins, such as collagen, fibronectin, and laminin, can also act to contract the aggregate of cells into a spheroid.[5] Once the cells of interest are grown into spheroids, there are several applications both *in vivo* and *in vitro*, including injection after an injury,[6] high-throughput assay to test compounds of interest,[7] and enhancement of microvessel formation.[8] Spheroids provide a three-dimensional (3D) niche that allows cells to interact with surrounding cells and ECM in all directions. The cells' microenvironment more closely mimics the *in vivo* conditions and is a vast improvement over traditional two-dimensional (2D) cell culture. Cells grown in this 3D microenvironment behave fundamentally differently from 2D-cultured cells. Numerous studies have shown that the biological properties of cells were significantly improved in spheroids compared to 2D-cultured cells. For example, primary hepatocytes and chondrocytes will lose their normal phenotype in monolayer culture, but this loss can be reversed simply by growing these cells into 3D spheroids.[9,10] Aggregation of cells such as myoblasts has also been shown to promote cell viability and proliferation.[11]

Human mesenchymal stem cells (hMSCs) are multipotent cells with many useful attributes such as their proliferative capacity *in vitro* and immunomodulatory abilities *in vivo*.[12–14] These cells can do more than simply respond to a stimulus and differentiate; they function as a source of cytokines and growth factors that can help injured tissue to recover.[15,16] Because hMSCs have immunomodulatory effects, allogeneic sources can be used without major immune reactions. hMSCs can be easily extracted and isolated from bone marrow and adipose tissue, and can be extensively expanded *in vitro*. However, the *in vitro* conventional 2D culture tends to cause hMSCs to differentiate and lose some of their advantageous regenerative and trophic properties. Culture of hMSCs into 3D spheroids provides a solution—hMSC spheroids exhibit greater cell proliferation, better preserved multilineage potential, and no cell necrosis when compared to traditional 2D monolayers.[5,17–20] In addition, hMSC spheroids can increase their ECM production

Department of Biomedical Engineering, Michigan Technological University, Houghton, Michigan.

and retention, anti-inflammatory activities, cell–cell contacts, and cell–ECM interactions.[19] These enhanced attributes can in turn improve implanted cell adhesion and retention, cell survival and long-term engraftment, leading to better hMSC therapeutic efficacy. hMSC spheroids have demonstrated positive outcomes in various preclinical studies, including bone and cartilage regeneration, wound healing, and neoangiogenesis.[5,17–20]

Physiological relevant low oxygen can maintain high progenicity and prevent differentiation of hMSCs.[21–23] In previous studies, it was shown that the physiologically low oxygen culture was able to stimulate hMSCs to express higher level of stem cell genes and produce more ECM proteins and angiogenic factors.[21–23] We hypothesize that the combination of low oxygen culture with the 3D environment of spheroid will better maintain the regenerative properties of hMSCs and significantly benefit their future clinical applications.

In this study, hMSC spheroids were cultured under several different conditions, varying culture time, and oxygen tension. ECM protein production, growth factor levels, and stemness of hMSCs were investigated under both normal oxygen (20%) and low oxygen (2%) at different time points. The reproducibility, attachment and spreading, and injectibility of hMSC spheroids were also tested to show their feasibility for *in vivo* usage.

Materials and Methods

Cell culture

The hMSCs and green fluorescent protein (GFP)-expressing hMSCs were obtained from Texas A&M University System Health Science Center. The passages four to five cells were used in this study. These cells were grown in a basal medium of α-Minimum Essential Medium (α-MEM) (Life Technologies, Carlsbad, CA) supplied with 1% L-glutamine (Life Technologies), 1% penicillin/streptomycin (Life Technologies), and 20% fetal bovine serum (FBS; Atlanta Biologicals, Norcross, GA). The hMSC spheroids were formed using a common and simple method—hanging drop method. This involves cells spontaneously aggregating at the bottom of a drop after inverting a plate with drops of cell suspension.[24] Briefly, after *in vitro* expansion, the cells were trypsinized and resuspended at a concentration of 400,000 cells/mL[24] in the basal medium containing 0.24% (w/v) methylcellulose (Sigma-Aldrich, St. Louis, MO). This cell suspension was then pipetted onto an inverted culture dish cover with 10 μL per droplet using a multichannel pipette. The dish cover was then turned over and placed back on the dish bottom, which contained sterile deionized (DI) water to reduce evaporation of the droplets. The culture time for the spheroids ranged from 24 to 96 h in low (2%) and normal oxygen (20%). Spheroids were then collected for various tests.

Human dermal fibroblast (hDF) cell sheets were used to mimic tissue *in vitro*. The hDFs were acquired from ATCC (Manassas, VA) and cultured in Dulbecco's modified Eagle's medium (DMEM) supplemented with 20% FBS, 20% Ham F12, 500 μM sodium ascorbate, and 1% penicillin/streptomycin (Life Technologies). Passages 3–4 hDFs were seeded on glass cover slides and grown for 48 h to form cell sheets.

DNA assay

DNA assay was performed as previously described.[25] Briefly, cells were lysed using the proteinase K solution (0.1 mg/mL) at 37°C for 2 h. Samples of 100 μL were placed in triplicate in a 96-well plate and mixed with 100 μL of PicoGreen (Life Technologies). The plate was incubated at room temperature for 10 min in the dark and then read on a Fluoroskan Ascent FL fluorescence plate reader (Thermo Fisher Scientific, Waltham, MA). A DNA standard curve was used to determine the levels of DNA in each sample.

Quantification of spheroid size

The spheroids were visualized using optical microscopy. The spheroid size was quantified and compared between the two oxygen conditions at different culture times. The Feret diameter was calculated for individual spheroid using the ImageJ software[26] (sample size = 100 spheroids per experimental group). The Feret diameter of a particle is the diameter measured at the maximum diameter. The circularity of each spheroid was determined using ImageJ. The Feret diameter was then obtained based on the statistical average diameter after rotating the circle 360° with 2° increments.

ECM and growth factor quantification

The ECM components in hMSC spheroids, including laminin, elastin, glycosaminoglycans (GAGs), and fibronectin, were examined. The growth factors, vascular endothelial growth factor (VEGF) and basic fibroblast growth factor (bFGF), were also tested. The elastin and GAG contents were quantified using colorimetric kits from Biocolor (UK). The laminin, fibronectin, VEGF, and bFGF were detected using *in situ* ELISA following our previous publication,[27] using primary antibodies and alkaline phosphatase-conjugated secondary antibody from Abcam (Cambridge, MA). Color intensities for blank, control, and experimental samples were

Table 1. Primer Sequences of Target Genes

Gene name	*Gene ID*	*Forward*	*Reverse*
Glyceraldehyde 3-phosphate dehydrogenase	GAPDH	5′-ACAGTTGCCATGTAGACC	5′-TTTTTGGTTGAGCACAGG
Octamer-binding transcription factor 4	POU5F1	5′-GATCACCCTGGGATATACAC	5′-GCTTTGCATATCTCCTGAAG
Rex1	ZFP-42	5′-GAATTCAGACCTAACCATCG	5′-TGAGCACTACTAGAGTGAAG
SRY (Sex Determining Region Y)-Box 2	SOX2	5′-ATAATAACAATCATCGGCGG	5′-AAAAAGAGAGGCAAACTG
Notch homolog 1, translocation-associated	Notch-1	5′-AAGATATGCAGAACAACAGG	5′-TCCATATGATCCGTGATGTC

recorded using a VERSA Max Tunable microplate reader (Molecular Devices, Sunnyvale, CA). The data were normalized to cell number in the hMSC spheroid.

Fluorescent imaging

Fluorescent staining was carried out on the samples after a 48-h incubation in 10% formalin. Spheroids were suspended in PolyFreeze (Polysciences, Inc., Warrington, PA) and sectioned to a thickness of 10 μm using a Microm HM 550 P cryostat (Waldorf, Germany). Samples were permeabilized using 0.2% (w/v) Triton-100 in phosphate-buffered saline (PBS) and blocked using a 1% (w/v) bovine serum albumin in PBS. Samples were incubated with primary antibodies for laminin, elastin, collagen I, and fibronectin (Abcam), overnight at 4°C followed by incubation in

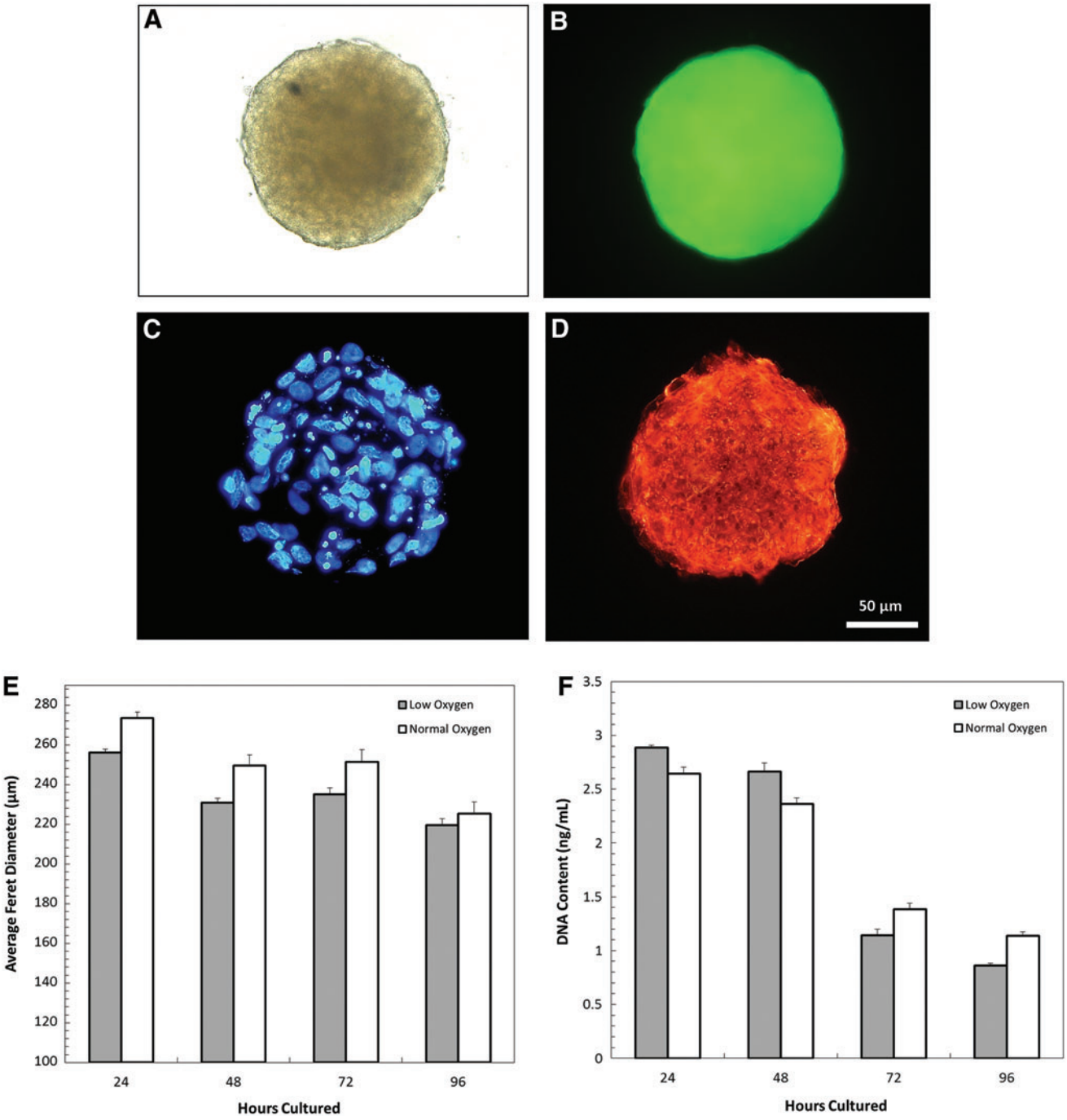

FIG. 1. The morphology of hMSC spheroids was observed through light microscopy **(A)**, GFP expression **(B)**, nucleus staining **(C)**, and F-actin staining **(D)**. The average Feret diameter and DNA content of hMSC spheroids cultured under low and normal oxygen conditions are shown in the **(E, F)**, respectively. No significant differences were found in both the Feret diameter and the DNA content between the two conditions. GFP, green fluorescent protein; hMSC, human mesenchymal stem cell. Color images available online at www.liebertpub.com/tec

the Alexa fluor 488 secondary antibody (Life Technologies) for 1 h. Nucleus staining was achieved using 4′,6-diamidino-2-phenylindole (DAPI). F-actin was visualized using rhodamine phalloidin. Fluorescent imaging utilized an Olympus BX-51 fluorescent microscope (Olympus America, Center Valley, PA).

Reverse transcription-polymerase chain reaction

After 72 h of culture, total RNA from different conditions was isolated using the RNeasy Mini kit (Qiagen, Valencia, CA). Reverse transcription (RT) was performed using 8 pg of total RNA with RT reaction mixture, which contains primers specific for stemness-related genes and normalized to housekeeping protein glyceraldehyde 3-phosphate dehydrogenase (GAPDH). The reverse transcription-polymerase chain reaction (RT-PCR was performed by StepOnePlus™ Real-Time PCR System (Applied Biosystems, Thermo Scientific) by means of SYBR® Green Real Time PCR Master Mixes (Life Technologies). The primer sequences of target genes are listed in Table 1.

Spheroid injection and spreading tests

The suspension of 1 mL of hMSC spheroids, which contained 400 spheroids, was injected through several sizes of needle gauges, including 18, 23, and 26 gauges. The cell morphology before and after injection was observed by staining cell nucleus and cytoskeleton protein F-actin. The DNA assay was also performed to confirm the spheroid integrity.

The hDF cell sheets were cultured for 48 h as described earlier in the Cell Culture section in a 12-well culture dish on circular glass coverslips (3.8 cm^2 growing area for each coverslip). A total of 100 spheroids were then placed in each well on the hDF cell sheets for 4 to 96 h. The morphology of spheroids was observed using fluorescent microscopy for F-actin and DAPI as described in the Fluorescent Imaging section.

Statistical methods

Quoted errors and error bars correspond to sample standard error. Beer's approach to the propagation of random errors[28] was used to calculate overall standard errors for DNA assay that took into account random error in measurements from the experimental group and background (blank) samples. p-Value used was <0.01.

Results

Formation of 3D hMSC spheroids

hMSC spheroids were fabricated through a hanging drop method and cultured for 24 to 96 h under both low oxygen

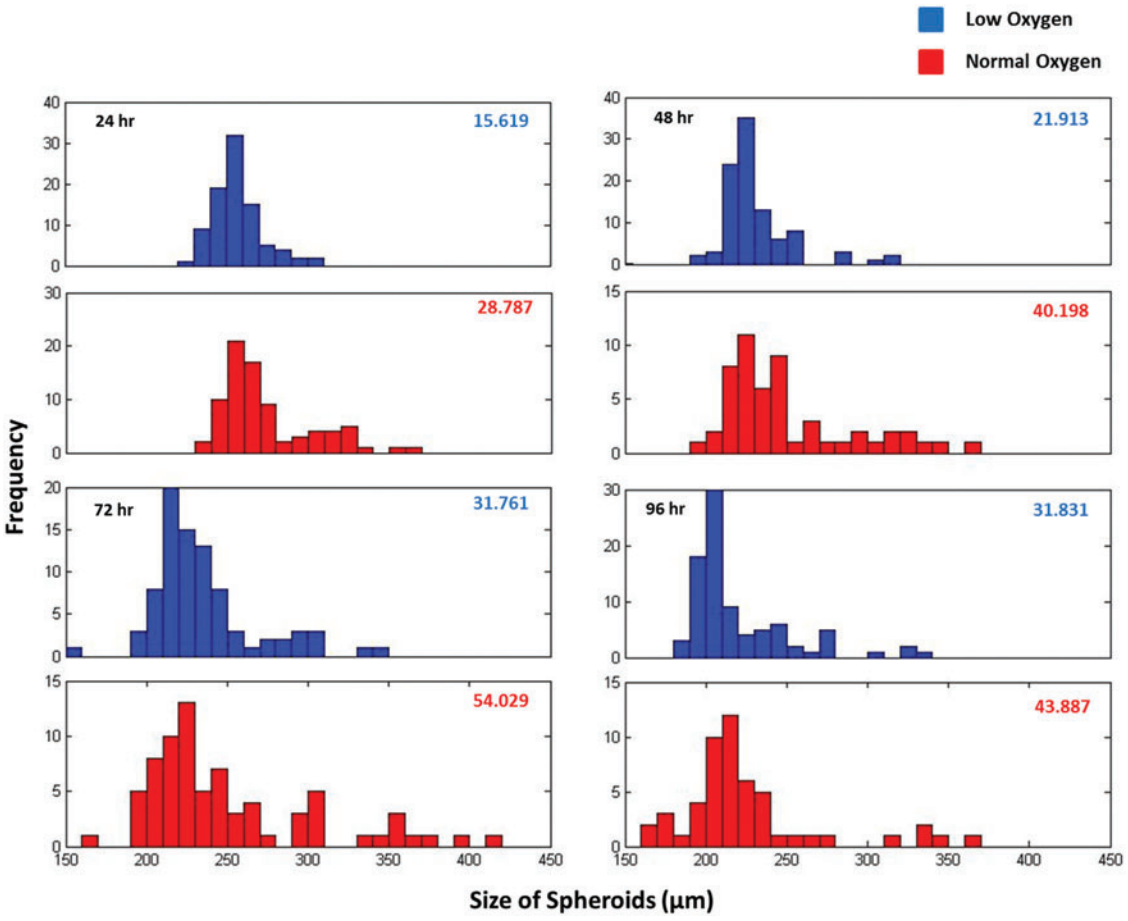

FIG. 2. Distribution of Feret diameter (μm) of hMSC spheroids cultured under low and normal oxygen conditions at different time points. Standard error for each condition is indicated in the *top right* corner of each plot. The hypoxia spheroids showed smaller variation at all time points. Color images available online at www.liebertpub.com/tec

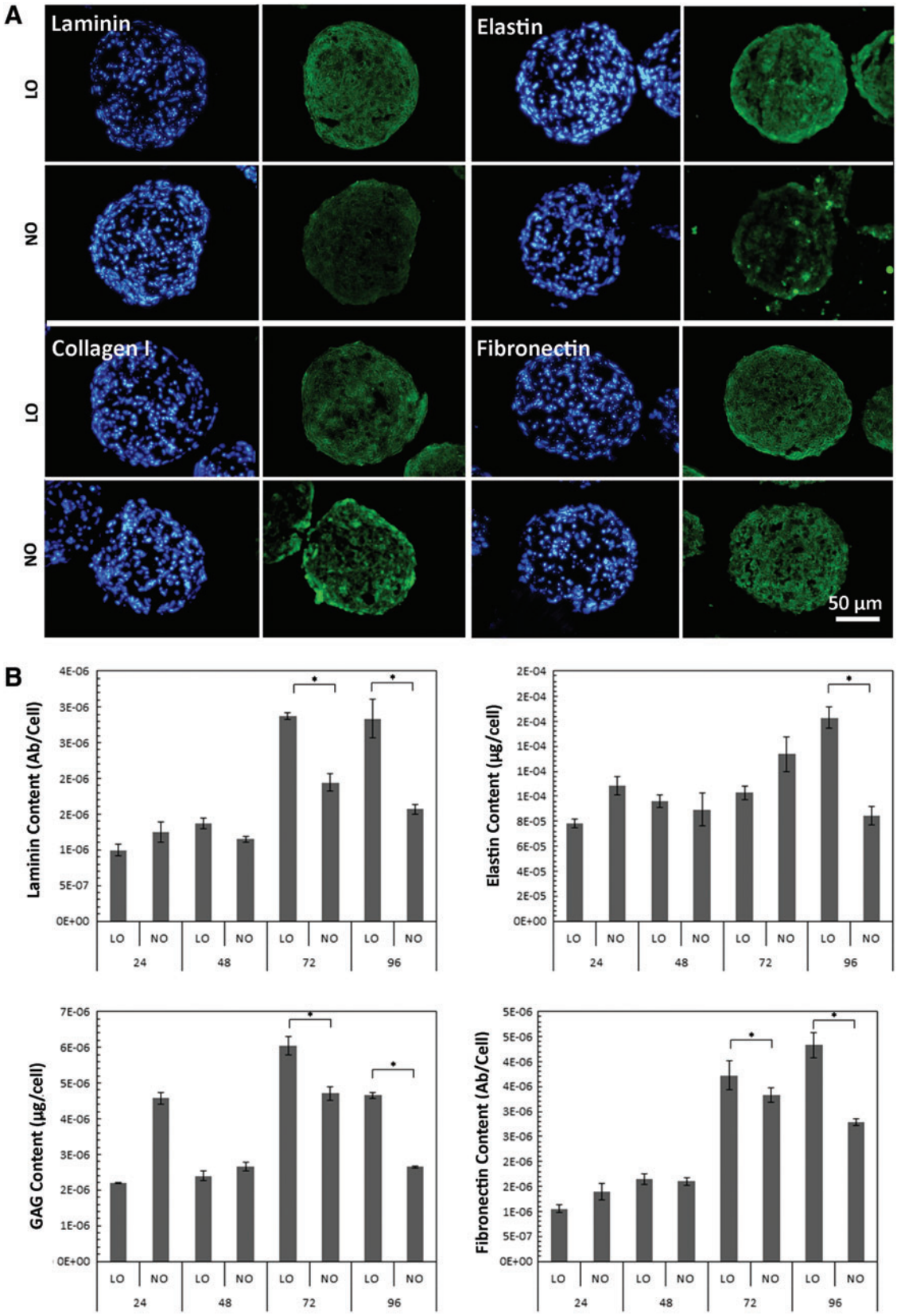

FIG. 3. ECM proteins laminin, elastin, collagen I, and fibronectin visualized using immunofluorescent staining (*green*) with nuclei stained with DAPI (*blue*) **(A)**. Quantification of ECM components laminin, elastin, glycosaminoglycan (GAG), and fibronectin **(B)**. Levels of these proteins were significantly higher in low oxygen compared to those in normal oxygen at later time points. $*p < 0.01$. DAPI, 4′,6-diamidino-2-phenylindole; ECM, extracellular matrix. Color images available online at www.liebertpub.com/tec

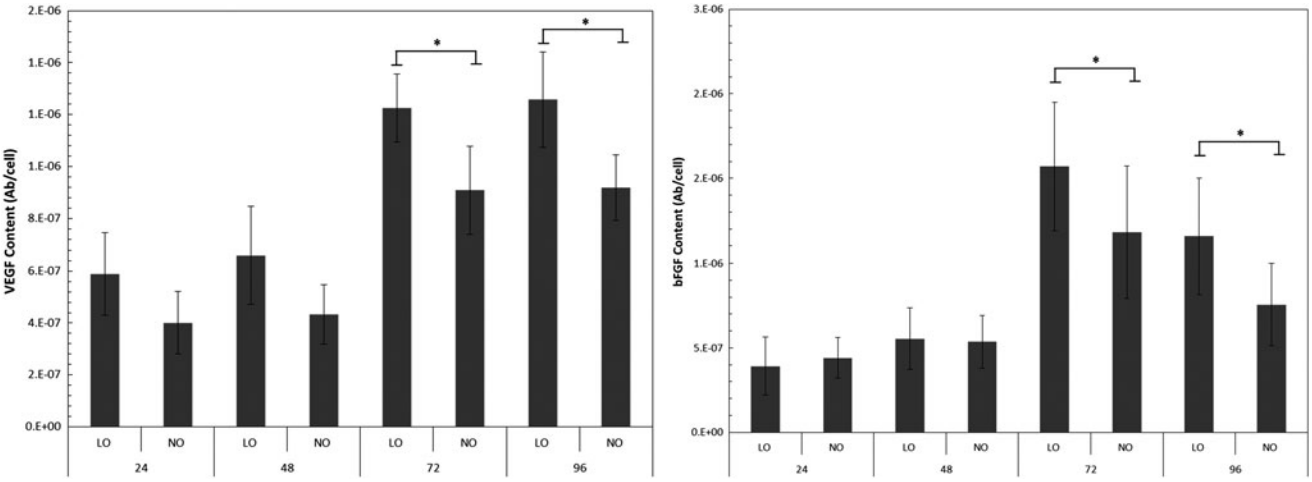

FIG. 4. Expression of growth factors VEGF and bFGF in hMSC spheroids cultured under low and normal oxygen conditions at different time points. Growth factor levels were significantly increased at 72 and 96 h under the low oxygen condition. $*p < 0.01$. bFGF, basic fibroblast growth factor; VEGF, vascular endothelial growth factor.

(2%) and normal oxygen (20%) conditions. Figure 1A shows the optical microscopy image of a single GFP-hMSC spheroid cultured under low oxygen for 72 h. Figure 1B–D shows the corresponding fluorescent images of the same spheroid. The cell nuclei were visualized with DAPI staining, cell body was visualized with GFP, and F-actin was shown with phalloidin staining. The cytoskeletal structure of the cells within the spheroid can be seen, indicating overall structural integrity. This shows the mechanical stability that the cytoskeleton provides to cells through the creation of complex F-actin networks. These crosslinked proteins confer viscoelastic properties to the individual cell and the overall spheroids as described by Lieleg *et al.*[29]

The average Feret diameter was determined using 100 spheroids per culture condition and is shown in Figure 1E. During the 96-h culture period, the hypoxia spheroids were smaller than normoxia spheroids, but there was no statistical difference between the average Feret diameters of these two conditions. The DNA content of the spheroids over time was also tested and shown in Figure 1F. The total number of cells decreased after 48 h, but again did not vary significantly between oxygen conditions. Feret diameter size distribution histograms of the spheroids from both culture conditions are shown in Figure 2, with standard error indicated in the corner of each graph. At all time points, the normal oxygen sample had a higher standard error and larger spread of the size distribution, particularly at 24 and 48 h. For both conditions, as culture time increased, the variability of the spheroid size increased.

ECM and growth factor production

ECM components, including laminin, elastin, collagen I, and fibronectin, were visualized by immunofluorescent staining after 72 h of culture from a spheroid cross section, as shown in Figure 3A. Appreciable levels of protein expression could be seen for each culture condition, demonstrating that the spheroids had ability to produce ECM even after a short culture period. ECM components laminin, elastin, GAGs, and fibronectin were also quantified for each culture condition, as shown in Figure 3B. Over time the ECM expression enhanced with over a twofold increase after 48 h for laminin, fibronectin, and GAGs, and approximately a 1.5-fold increase for elastin. At 72 and 96 h, all the tested ECM component levels were significantly higher in the low oxygen condition in comparison to normal oxygen condition.

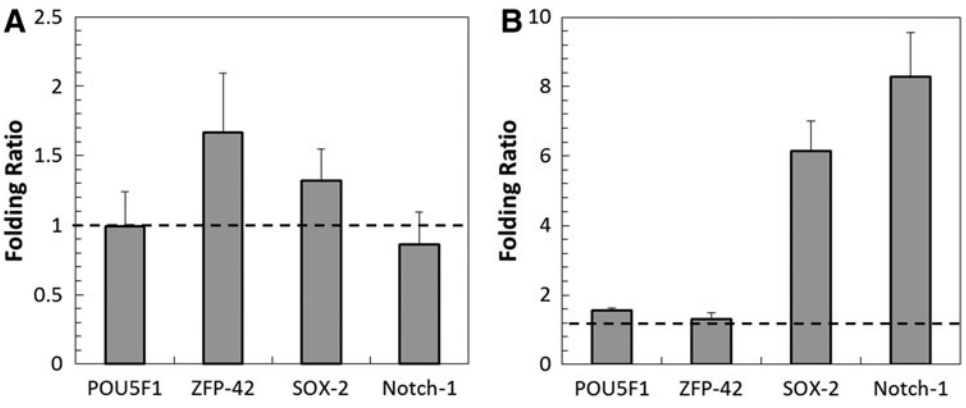

FIG. 5. Expression of stem cell genes in hMSC spheroids cultured under low and normal oxygen at 72 h **(A)**. Expression of stem cell genes in low oxygen hMSC spheroids compared to normal oxygen hMSCs cultured on flat substrate at 72 h **(B)**. Folding ratios for **(A)** were close to 1, indicating very little difference in gene expression. The SOX-2 and Notch-1 showed a higher gene expression in low oxygen spheroids compared to flat normal oxygen cultures in **(B)**.

VEGF and bFGF were also quantified using *in situ* ELISA and shown in Figure 4. Similar to the ECM expression trend, the level of growth factor production in the spheroids increased as culture time increased. Also, hypoxia spheroid had significantly higher levels of growth factors compared to normal oxygen samples at 72 and 96 h, with a 1.3-fold increase in both VEGF and bFGF.

Stemness of hMSC spheroids

Stemness of the hMSC spheroids was assessed by four stem cell markers: POU5F1 (octamer-binding transcription factor, OCT-4), ZFP-42 (REX-1), SOX-2 (sex determining region Y-box 2), and Notch-1. Folding ratios are shown in Figure 5. Panel A indicates the ratio of normal oxygen spheroids to low oxygen spheroids (72 h). All ratios are fairly close to 1, and therefore, there was not a large difference in gene expression between the two oxygen conditions. The low oxygen spheroids were also compared to the normal oxygen hMSCs grown on a flat culture plate, as shown in Figure 5B. Both SOX-2 and Notch-1 genes had much higher folding ratios, indicating a higher expression in the low oxygen spheroids. POU5F1 and ZFP-42 are both close to 1, and therefore, there was not a large difference in those gene expressions.

Injectibility of hMSC spheroids

One possible application of these hMSC spheroids is injection into wound sites to facilitate healing. Therefore, it is important to test how they hold up to different gauges of needle after injection. Different needles (18, 23, and 26 gauge) were used to inject the spheroids, and F-actin and nuclei were visualized using fluorescent imaging to ensure no gross defects occurred as a result of being injected. Both hypoxia and normoxia spheroids appeared as a complete and undamaged structure compared to control spheroids, suggesting that no gross defects occurred after injection. The DNA content was also tested using 72-h hMSC spheroids with a DNA assay, as shown in Figure 6B. The DNA assay demonstrates that for all gauge sizes and oxygen conditions, the cell numbers were not significantly different from each other.

hMSC spheroid attachment and spreading

The next step was to simulate the spheroid attachment to model tissues after injection using a hDF cell sheet. hDF cells were grown into a confluent sheet after 48 h of culture. GFP-hMSCs[30] were used to track cells as they attached and spread on the hDF tissue substitute, which was stained to visualize the cell nuclei and F-actin, as seen in Figure 7A. Panel B shows the hypoxia spheroid before placement on tissue substitute, and Panel C and D of Figure 7 show the morphology of cell sheet and spheroid after 72 h of coculture. The spheroid had begun to spread over the surface of the hDF cell sheet, and individual GFP-hMSCs could be seen migrating away from the original spheroid.

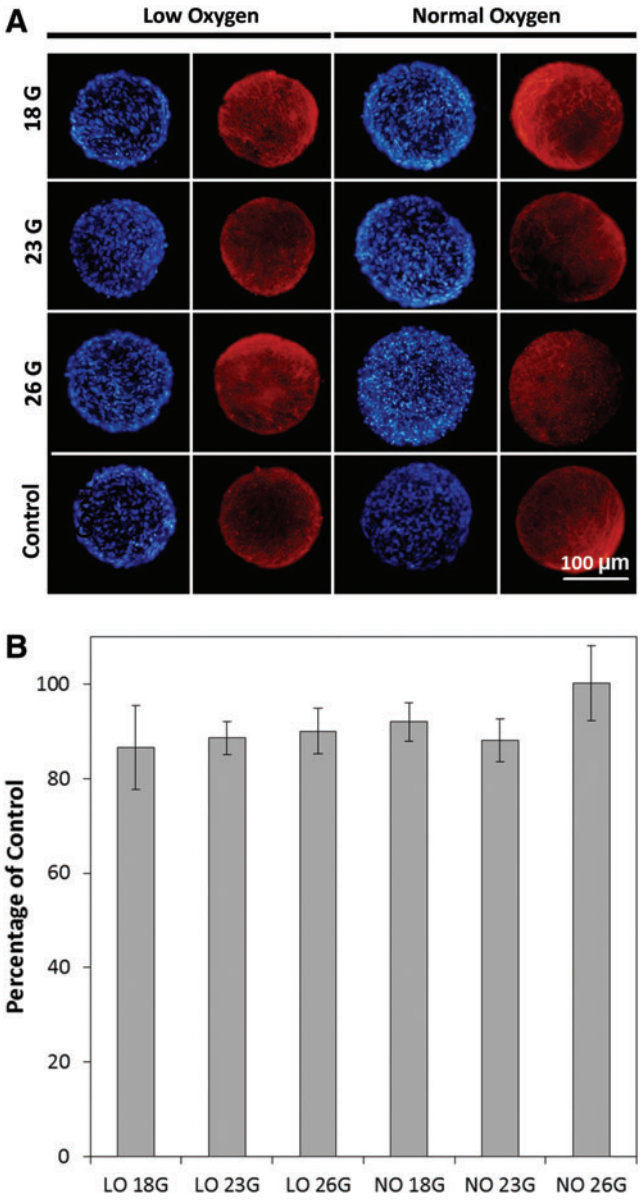

FIG. 6. Injectibility of hMSC spheroids cultured under low and normal oxygen conditions tested using needles with different gauge sizes, including 18, 23, and 26 gauges. The F-actin (*red*) and cell nuclei (*blue*) were stained to observe the spheroid morphology **(A)**. hMSC spheroids appeared undamaged after injection conditions. The DNA assay showed that there was no significant difference in the DNA content among all the culture conditions **(B)**. Color images available online at www.liebertpub.com/tec

Discussion

Multicellular hMSC spheroids have been shown to have many useful applications such as cartilage regeneration, wound healing, and neoangiogenesis.[5,17,18] 3D culture systems more accurately reflect *in vivo* gene expression profiles and therefore help to preserve many of the valuable attributes of hMSCs. Also, 3D spheroids create more cell–cell and cell–ECM interactions, while maintaining a small enough tissue construct that diffusion of oxygen and waste products is not a concern.[1] However, the hMSCs cultured under normal oxygen conditions tend to differentiate and lose progenicity. Low oxygen can help to maintain the stemness of hMSCs in different 2D and 3D culture systems. Culture of hMSC spheroids under the hypoxia condition

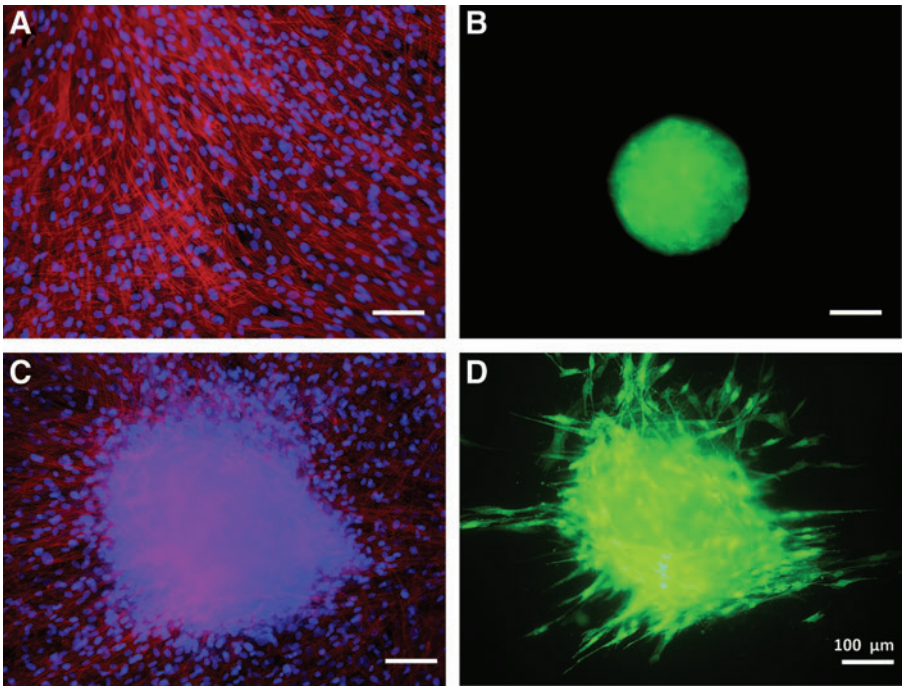

FIG. 7. Attachment of hypoxia GFP-hMSC spheroids on model tissue substitute-hDF cell sheet. **(A, B)** The morphology of fibroblast cell sheet and spheroid before attachment. F-actin (*red*), cell nuclei (*blue*), GFP (*green*). **(C, D)** The cell sheet and spheroid after 72 h of coculture with spreading of the GFP-hMSCs. hDF, human dermal fibroblast. Color images available online at www.liebertpub.com/tec

may better preserve hMSC regenerative properties, thus enhancing the therapeutic efficacy.

ECM plays a vital role in both structure and organization of tissue constructs. ECM component levels were evaluated for several time points under low and normal oxygen conditions. Over time, ECM levels increased during the initial stages of culture for both oxygen conditions.[31] At 72 and 96 h, ECM levels were significantly increased in the low oxygen condition, as shown in Figure 3, which was consistent with previous studies. For example, hMSCs cultured on 2D polydimethylsiloxane and 3D polyethylene terephthalate substrates under 2% O_2 expressed much higher fibronectin than those cultured under 20% O_2.[22,23] Higher levels of ECM in spheroids were linked to enhanced apoptosis resistance both in cell culture and after implantation *in vivo*.[32,33] Increased fibronectin, laminin, and collagen I were associated with a larger number of attached and integrated spheroids as well.[34–36] The presence of fibronectin, laminin, collagen, and GAGs was also desirable to mimic the cell conditions *in vivo* and therefore served as a better model environment for high-throughput assay.[37] All of these ECM components were found in detectable levels in the hMSC spheroids, with levels increasing under low oxygen at later time points.

VEGF and bFGF are important growth factors regulating cell proliferation, angiogenesis, and other cellular behavior. VEGF is well known to mediate angiogenic and lymphangiogenic activity during the proliferative phase of wound healing, which is an essential component of normal wound repair.[38] The presence of VEGF was able to promote the resolution of chronic wounds (often associated with diabetes) exhibiting compromised vascularity.[39] bFGF was also linked to acceleration of wound healing through stimulation of ECM metabolism and cell migration.[40,41] Increased levels of these growth factors made hypoxia spheroids better candidates for wound healing applications. VEGF and bFGF showed similar expression patterns in hMSC spheroid culture. Hypoxia hMSC spheroids expressed much higher growth factors (around 1.3-fold increase) at later time points than normoxia spheroids. This increase was similar to levels reported by Lee *et al* with a 2.8- and 2.3-fold increase of VEGF and bFGF, respectively, for adipose-derived stem cells under 2% oxygen flat culture for 72 h.[42] The hypoxic treatment of hMSCs also significantly increased VEGF by 2.56 fold and bFGF expression by 3.33 fold.[43] VEGF had also been shown to be increased in spheroids formed on chitosan films for 7 days, with a 1.2-fold increase in VEGF, but with no significant change in bFGF.[44] This increase of growth factors due to low oxygen culture and 3D condition could in turn activate the collagen synthesis and migration of fibroblasts, leading to enhanced wound healing.[45]

Well-maintained stemness is essential for clinical applications of hMSCs. The cells must maintain their multipotency until implantation so they can respond to the local microenvironment and receive site-specific cues for differentiation. Our results demonstrated that all of the four stemness markers OCT-4 (POU5F1), Rex-1 (ZFP-42), SOX-2, and Notch-1 levels did not change significantly in spheroids between different oxygen culture conditions. However, compared to flat substrate culture, SOX-2 and Notch-1 gene expression was increased dramatically in low oxygen spheroids. Although both 3D spheroids and low oxygen culture could enhance hMSC stemness gene expression when compared to flat substrate culture, the combination of these two favorable conditions was not able to further significantly increase the hMSC stemness. The possible reason was that the hMSC stemness was well maintained in spheroids, and it is difficult to make improvement during a hypoxia culture period as short as 96 h.

The ability to maintain integrity after injection and the ability to attach to a model tissue substrate are important for the future clinical application of hMSC spheroids. Even using the smallest gauge needle, 26G, there was no visible damage for both low and normal oxygen samples at 72 h. There was also no change in cell number for different needle

gauges as shown in Figure 6. These properties demonstrated the spheroids' ability to withstand the stress of injection into sites of interest *in vivo*. Attachment and spreading of the spheroids were also investigated using a hDF cell sheet as a tissue substitute. GFP-hMSC low oxygen spheroids were able to attach even within 2 h, and after 72 h, significant spreading occurs, as seen in Figure 7. The ability to attach and integrate within tissues was essential to many *in vivo* applications of hMSC spheroids.

Conclusions

hMSC multicellular spheroids were fabricated through the hanging drop method, and low oxygen condition was used to enhance essential properties of these spheroids. The spheroids' size and cell proliferation did not vary significantly at each time point for low and normal oxygen culture condition. However, hypoxia spheroids demonstrated lower variability than normoxia samples. The hypoxia spheroids also produced higher amount of ECM components (including fibronectin, laminin, elastin, and GAGs) and growth factors (VEGF and bFGF). Stemness of hMSCs was maintained in hypoxia spheroids and much higher than flat hMSC culture at normal oxygen. The hypoxia spheroid structural integrity and cell number were maintained after injection. The hypoxia spheroids also demonstrated ability to attach and spread on a tissue substitute *in vitro*. Our results suggested that the hypoxia hMSC spheroids may have better regeneration capacity for future *in vivo* applications.

Acknowledgments

This study was supported by the National Institutes of Health (1R15HL115521-01A1) and the Research Excellence Fund-Research Seed Grant (REF-RS) from Michigan Technological University to F.Z.

Disclosure Statement

No competing financial interests exist.

References

1. Fennema, E., Rivron, N., Rouwkema, J., van Blitterswijk, C., and de Boer J. Spheroid culture as a tool for creating 3D complex tissues. Trends Biotechnol **31,** 108, 2013.
2. Dean, D.M., Napolitano, A.P., Youssef, J., and Morgan, J.R. Rods, tori, and honeycombs: the directed self-assembly of microtissues with prescribed microscale geometries. FASEB J **21,** 4005, 2007.
3. Achilli, T.M., Meyer, J., and Morgan, J.R. Advances in the formation, use and understanding of multi-cellular spheroids. Expert Opin Biol Ther **12,** 1347, 2012.
4. Foty, R.A., and Steinberg, M.S. The differential adhesion hypothesis: a direct evaluation. Dev Biol **278,** 255, 2005.
5. Bhang, S.H., Cho, S.W., La, W.G., Lee, T.J., Yang, H.S., Sun, A.Y., *et al.* Angiogenesis in ischemic tissue produced by spheroid grafting of human adipose-derived stromal cells. Biomaterials **32,** 2734, 2011.
6. Peura, M., Bizik, J., Salmenpera, P., Noro, A., Korhonen, M., Patila, T., *et al.* Bone marrow mesenchymal stem cells undergo nemosis and induce keratinocyte wound healing utilizing the HGF/c-Met/PI3K pathway. Wound Repair Regen **17,** 569, 2009.
7. Kunz-Schughart, L.A., Freyer, J.P., Hofstaedter, F., and Ebner, R. The use of 3-D cultures for high-throughput screening: the multicellular spheroid model. J Biomol Screen **9,** 273, 2004.
8. Laib, A.M., Bartol, A., Alajati, A., Korff, T., Weber, H., and Augustin, H.G. Spheroid-based human endothelial cell microvessel formation in vivo. Nat Protoc **4,** 1202, 2009.
9. Bierwolf, J., Lutgehetmann, M., Feng, K., Erbes, J., Deichmann, S., Toronyi, E., *et al.* Primary rat hepatocyte culture on 3D nanofibrous polymer scaffolds for toxicology and pharmaceutical research. Biotechnol Bioeng **108,** 141, 2011.
10. von der Mark, K., Gauss, V., von der Mark, H., and Muller, P. Relationship between cell shape and type of collagen synthesized as chondrocytes lose their cartilage phenotype in culture. Nature **267,** 531, 1977.
11. Bayoussef, Z., Dixon, J.E., Stolnik, S., and Shakesheff, K.M. Aggregation promotes cell viability, proliferation, and differentiation in an in vitro model of injection cell therapy. J Tissue Eng Regen Med **6,** e61, 2012.
12. Wagner, J., Kean, T., Young, R., Dennis, J.E., and Caplan, A.I. Optimizing mesenchymal stem cell-based therapeutics. Current Opin Biotechnol **20,** 531, 2009.
13. Caplan, A.I., and Correa, D. The MSC: an injury drugstore. Cell Stem Cell **9,** 11, 2011.
14. Groh, M.E., Maitra, B., Szekely, E., and Koc, O.N. Human mesenchymal stem cells require monocyte-mediated activation to suppress alloreactive T cells. Exp Hematol **33,** 928, 2005.
15. Caplan, A.I., and Dennis, J.E. Mesenchymal stem cells as trophic mediators. J Cell Biochem **98,** 1076, 2006.
16. Haynesworth, S.E., Baber, M.A., and Caplan, A.I. Cytokine expression by human marrow-derived mesenchymal progenitor cells in vitro: effects of dexamethasone and IL-1 alpha. J Cell Physiol **166,** 585, 1996.
17. Suzuki, S., Muneta, T., Tsuji, K., Ichinose, S., Makino, H., Umezawa, A., *et al.* Properties and usefulness of aggregates of synovial mesenchymal stem cells as a source for cartilage regeneration. Arthritis Res Ther **14,** R136, 2012.
18. Amos, P.J., Kapur, S.K., Stapor, P.C., Shang, H., Bekiranov, S., Khurgel, M., *et al.* Human adipose-derived stromal cell accelerate diabetic wound healing: impact of cell formulation and delivery. Tissue Eng Part A **16,** 808, 2010.
19. Sart, S., Tsai, A.C., Li, Y., and Ma, T. Three-dimensional aggregates of mesenchymal stem cells: cellular mechanisms, biological properties, and applications. Tissue Eng Part B Rev **20,** 365, 2014.
20. Tsai, A.C., Liu, Y., Yuan, X., and Ma, T. Compaction, fusion, and functional activation of three-dimensional human mesenchymal stem cell aggregate. Tissue Eng Part A **21,** 1705, 2015.
21. Grayson, W.L., Zhao, F., Bunnell, B., and Ma, T. Hypoxia enhances proliferation and tissue formation of human mesenchymal stem cells. Biochem Biophys Res Commun **358,** 948, 2007.
22. Grayson, W.L., Zhao, F., Izadpanah, R., Bunnell, B., and Ma, T. Effects of hypoxia on human mesenchymal stem cell expansion and plasticity in 3D constructs. J Cell Physiol **207,** 331, 2006.
23. Zhao, F., Veldhuis, J.J., Duan, Y., Yang, Y., Christoforou, N., Ma, T., *et al.* Low oxygen tension and synthetic nanogratings improve the uniformity and stemness of human mesenchymal stem cell layer. Mol Ther **18,** 1010, 2010.

24. Hutton, D.L., Moore, E.M., Gimble, J.M., and Grayson, W.L. Platelet-derived growth factor and spatiotemporal cues induce development of vascularized bone tissue by adipose-derived stem cells. Tissue Eng Part A **19,** 2076, 2013.
25. Xing, Q., Vogt, C., Leong, K.W., and Zhao, F. Highly aligned nonfibrous scaffold derived from decellularized human fibroblasts. Adv Funct Mater **24,** 3027, 2014.
26. Schneider, C.A., Rasband, W.S., and Eliceiri, K.W. NIH Image to ImageJ: 25 years of image analysis. Nat Methods **9,** 671, 2012.
27. Xing, Q., Yates, K., Tahtinen, M., Shearier, E., Qian, Z., and Zhao, F. Decellularization of fibroblast cell sheets for natural extracellular matrix scaffold preparation. Tissue Eng Part C **21,** 77, 2015.
28. Beers, Y. Introduction to the Theory of Error. 2nd ed. Reading, MA: Addison-Wesley, 1957.
29. Lieleg, O., Claessens, M.M., and Bausch, A.R. Structure and dynamics of cross-linked actin networks. Soft Matter **6,** 218, 2010.
30. Prendergast, F.G., and Mann, K.G. Chemical and physical properties of aequorin and the green fluorescent protein isolated from Aequorea forskalea. Biochemistry **17,** 3448, 1978.
31. Mather, J.P. Extracellular Matrix. Stem Cell Culture: Methods in Cell Biology. Burlingham, MA: Academic Press, 2011, p. 174–175.
32. Santini, M.T., Rainaldi, G., and Indovina, P.L. Apoptois, cell adhesion, and the extracellular matrix in the three-dimensional growth of multicellular spheroids. Crit Rev Oncel Hematol **36,** 75, 2000.
33. Zahir, N., and Weaver, V.M. Death in the third dimension: apoptosis regulation and tissue architecture. Curr Opin Genet Dev **14,** 71, 2004.
34. Indovina, P., Rainaldi, G., and Santini, M.T. Hypoxia increases adhesion and spreading of MG-63 three-dimensional tumor spheroids. Anticancer Res **28,** 1013, 2008.
35. Inamori, M., Mizumoto, H., and Kajiwara, T. An approach for formation of vascularized liver tissue by endothelial cell-covered hepatocyte spheroid integration. Tissue Eng Part A **15,** 2029, 2009.
36. Mahesparan, R., Read, T.-A., Lund-Johnson, M., Skaftnesmo, K.O., Bjerkvig, R., and Engebraaten, O. Expression of extracellular matrix components in a highly infiltrative in vivo glioma model. Acta Neuropathol **105,** 49, 2003.
37. Nederman, T., Norling, B., Glimelius, B., Carlsson, J., and Brunk, U. Demonstration of an extracellular matrix in multicellular tumor spheroids. Cancer Res **44,** 3090, 1984.
38. Nissen, N.N., Polverini, P.J., Koch, A.E., Volin, M.V., Gamelli, R.L., and DiPietro, L.A. Vascular endothelial growth factor mediates angiogenic activity during the proliferative phase of wound healing. Am J Pathol **152,** 1445, 1998.
39. Bao, P., Kodra, A., Tomic-Canic, M., Golinko, M.S., Ehrlich, H.P., and Brem, H. The role of vascular endothelial growth factor in wound healing. J Surg Res **153,** 347, 2009.
40. McGee, G.S., Davidson, J.M., Buckley, A., Sommer, A., Woodward, S.C., Aquino, A.M., *et al.* Recombinant basic fibroblast growth factor accelerates wound healing. J Surg Res **45,** 145, 1988.
41. Hebda, P.A., Klingbeil, C.K., Abraham, J.A., and Fiddes, J.C. Basic fibroblast growth factor stimulation of epidermal wound healing in pigs. J Invest Dermat **95,** 626, 1990.
42. Lee, E.Y., Xia, Y., Kim, W.-S., Kim, M.H., Kim, T.H., Kim, K.J., *et al.* Hypoxia-enhanced wound-healing function of adipose-derived stem cells: increase in stem cell proliferation and up-regulation of VEGF and bFGF. Wound Repair Regen **17,** 540, 2009.
43. Chen, L., Xiu, Y., Zhao, J., Zhang, Z., Yang, R., Xie, J., Xusheng, L., and Qi, S. Conditioned medium from hypoxic bone marrow-derived mesenchymal stem cells enhances wound healing in mice. PLoS One **9,** e96161, 2014.
44. Cheng, N.C., Chen, S.Y., Li, J.R., and Young, T.H. Short-term spheroid formation enhances the regenerative capacity of adipose-derived stem cells by promoting stemness, angoigenesis, and chemotaxis. Stem Cells Trans Med **2,** 584, 2013.
45. Barrientos, S., Stojadinovic, O., Golinko, M.S., Brem, H., and Tomic-Canic, M. Growth factors and cytokines in wound healing. Wound Repair Regen **16,** 585, 2008.

Address correspondence to:
Feng Zhao, PhD
Department of Biomedical Engineering
Michigan Technological University
1400 Townsend Drive
Houghton, MI 49931-1295

E-mail: fengzhao@mtu.edu

Received: October 13, 2015
Accepted: January 27, 2016
Online Publication Date: March 21, 2016